Structural evolution and medium-temperature thermochronology of central Madagascar: implications for Gondwana amalgamation

Sheree E. Armistead[a*], Alan S. Collins[a], Ahmad Redaa[a,b], Sarah Gilbert[a], Gilby Jepson[a], Jack Gillespie[a], Morgan L. Blades[a], John D. Foden[a], Théodore Razakamanana[c]

[a]Centre for Tectonics, Resources and Exploration (TRaX), Department of Earth Sciences, The University of Adelaide, SA 5005, Australia

[b]Faculty of Earth Sciences, King Abdulaziz University, Jeddah, Saudi Arabia

[c]Département des Sciences de la Terre, Université de Toliara, Toliara, Madagascar

*correspondence: sheree.armistead@adelaide.edu.au

Abstract

Madagascar occupied an important place in the amalgamation of Gondwana, and preserves a record of several Neoproterozoic events that can be linked to orogenesis of the East African Orogen. We integrate remote sensing and field data to unravel complex deformation in the Ikalamavony and Itremo domains of central Madagascar. The deformation sequence comprises a gneissic foliation (S1), followed by south to south-west directed, tight to isoclinal, recumbent folding (D2). These are overprinted by north-trending upright folds that formed during a ~E–W shortening event. Together these produced type 1 and type 2 fold interference patterns throughout the Itremo and Ikalamavony domains. Apatite U–Pb and muscovite and biotite Rb–Sr thermochronometers indicate that much of central Madagascar was thermally reset to at least ~500^{o}C at c. 500 Ma. Deformation in west-central Madagascar occurred between c. 750 Ma and c. 550 Ma, and we suggest this deformation formed in response to the c. 650 Ma collision of Azania with Africa along the Vohibory Suture in southwestern Madagascar. In eastern Madagascar, deformation is syn- to post-550 Ma, which formed in response to the final closure of the Mozambique Ocean along the Betsimisaraka Suture that amalgamated Madagascar with the Dharwar Craton of India.

Keywords: thermochronology, Gondwana, remote sensing, GIS, supercontinents

Supplementary material:

Supplementary A: Detailed methodology and geo/thermochronology results

Supplementary B: Isotopic data for geo/thermochronology

1. Introduction

The amalgamation of central Gondwana occurred through convergence at several discrete subduction and collisional zones; collectively forming the East African Orogen. Madagascar was located in the centre of Gondwana and provides an ideal natural laboratory to study how this supercontinent coalesced (Collins, 2006; Collins and Windley, 2002; Tucker et al., 1999). Of particular interest and contention, is how and when the Archaean nucleus of Madagascar amalgamated with the Dharwar Craton of India to the east, and East Africa to the west, as well as smaller continental blocks of equivocal origin. Reconciling this tectonic history has major implications for global plate tectonic models during the Neoproterozoic (e.g. Merdith et al., 2017).

Madagascar is made up of several terranes ranging in age from Archaean to recent (Figure 1b). The centre of Madagascar is made up of the Antananarivo Domain, which comprises c. 2500 Ma magmatic gneisses (Collins and Windley, 2002; Kröner et al., 2000; Tucker et al., 1999). To the east of this craton are the Antongil and Masora cratons. These contain gneisses that are c. 3100 Ma and c. 2500 Ma, and are interpreted as a continuation of the Dharwar Craton of India (Armistead et al., 2017; Schofield et al., 2010; Tucker et al., 1999). Along the southwest margin of the Antananarivo Craton is the Itremo Group (Figure 2), made up of quartzites, schists and marbles with a maximum depositional age of c. 1600 Ma (Costa et al., Submitted; Cox et al., 1998; Fernandez et al., 2003). To the southwest of the Itremo Group, is the Ikalamavony Group, similarly made up of quartzites, schists and marbles but with a maximum depositional age of c. 1000 Ma. To the south of these metasedimentary terranes are the Proterozoic Anosyen, Androyen and Vohibory terranes (Boger et al., 2014; Emmel et al., 2008; Jöns and Schenk, 2007). In northern Madagascar is the c. 800–700 Ma Bemarivo Belt, which likely formed as an exotic juvenile arc terrane that amalgamated with Madagascar at c. 520 Ma (Armistead et al., In Review; Thomas et al., 2009).

The central Madagascan terranes discussed in this paper are bounded by two major sutures; the eastern Betsimisaraka Suture and the western Vohibory Suture. These may have resulted from at least two distinct major orogenic events that resulted in the amalgamation of Madagascar, the Dharwar Craton of India and Africa (Figure 1). However, the timing, location, and direction of subduction leading to these orogenic events remain contentious. Two end-member models are generally evaluated for the amalgamation of Madagascar; 1) that the Dharwar–central Madagascar collision (eastern suture) occurred in the late Archaean, and that central Madagascar and the Dharwar craton existed as “the Greater Dharwar Craton” through the entire Proterozoic eon (Tucker et al., 2011), and that widespread Neoproterozoic–Cambrian magmatism and metamorphism in Madagascar resulted from Madagascar–Africa collision (western suture); or 2) that the Dharwar Craton and central Madagascar were separate terranes that were sutured during a major Ediacaran–Cambrian East African orogenic event (the Malagasy Orogeny of Collins and Pisarevsky 2005), marked by the Betsimisaraka Suture in eastern Madagascar (Figure 1b). In this model, the central Madagascar–Africa collision occurred at c. 650–630 Ma (Armistead et al., 2017; Collins and Pisarevsky, 2005; Collins and Windley, 2002; Emmel et al., 2008) as the East African Orogeny. Other authors have suggested a c. 750–650 Ma age for the eastern suture (Fitzsimons and Hulscher, 2005), a c. 850–750 Ma age for the western suture (Moine et al., 2014), or even a c. 550 Ma age for the western suture (Boger et al., 2014; Jöns and Schenk, 2011). The proximity of these two suture zones makes it difficult to unravel the timing of events, as more recent events have the potential to overprint and obliterate the record of earlier events, such as through high temperature resetting of key minerals used for thermochronology and metamorphism.

The cross-cutting relationships and deformation history of the terranes that make up Madagascar can provide clues as to the timing of major orogenic events in Madagascar. Here we use structural geology to understand the deformation history of central Madagascar, which encompasses the two hypothesised suture zones. We have also collected U–Pb zircon, U–Pb apatite, Rb–Sr muscovite and Rb–Sr biotite thermochronology data to provide some absolute timing constraints on deformation in the region.

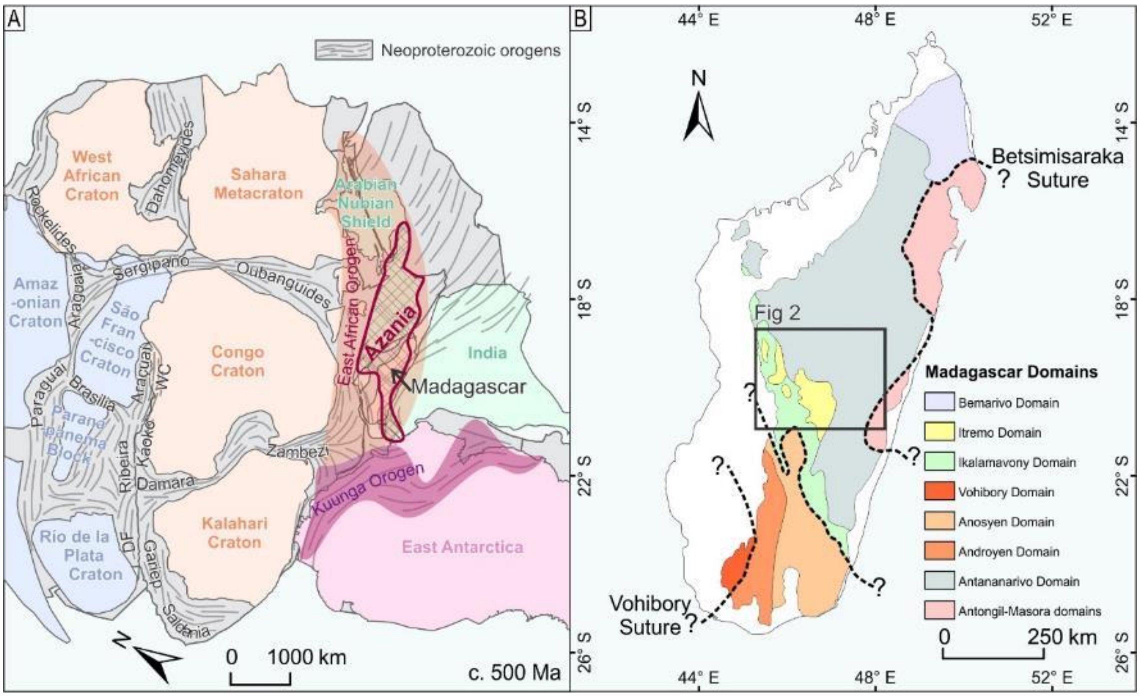

Figure 1 a) Tectonic map of Gondwana made using GPlates exported geometries from Merdith et al. (2017) in ArcGIS; projected in Hotine Oblique Mercator with Madagascar in the centre (reconstructed position, longitude=-75 and latitude=+40). DF= Dom Feliciano Belt, WC= West Congo; b) Present day map of the geological domains of Madagascar after (De Waele et al., 2011), possible suture zones shown by dashed lines, study area outlined in grey.

1.1 Regional structural and geochronological framework for central Madagascar

This study focuses on central Madagascar including parts of the Ikalamavony, Itremo and Antananarivo domains, between the two major suture zones in Madagascar (Figure 1; Figure 2). Structural geology and various geochronological methods are used to define and distinguish orogenic events in this central Madagascar. Although several structural studies from other key regions in Madagascar have been undertaken, very little work has been done on this region where the focus is on Neoproterozoic deformation and its association with collisional events.

Collins et al. (2003b) and Tucker et al. (2007) undertook comprehensive studies of the structure of the Itremo Group in central Madagascar. This area contains spectacularly folded sequences visible from satellite imagery (Figure 5). Collins et al. (2003b) interpreted a D1 event that produced 10 km scale recumbent, isoclinal folding predating c. 800–780 Ma intrusive rocks of the Imorona-Itsindro Suite. D2 was interpreted as a local deformation event that occurred synchronously with c. 800–780 Ma intrusions. D3 was interpreted as an east-west shortening event with thrusting and at least two phases of upright folding. D4 is expressed as post-550 Ma normal shearing and marks the boundary between the Itremo Group and Antananarivo Craton (Betsileo Shear Zone; Collins et al. 2000). Tucker et al. (2007) interpreted a similar history for the Itremo group with km-scale fold and thrust nappes, and east-directed vergence. This resulted in inversion and repetition of the Archaean Antananarivo gneisses and the Proterozoic Itremo Group, with hot (old) rocks being thrust over cool (young) rocks. This was followed by east-west shortening that resulted in upright folding of nappes to produce km-scale fold interference patterns. This event occurred within a sinistral transpressive regime and was associated with the Ranotsara Shear Zone in southern Madagascar (Tucker et al., 2007). These two models for the Itremo Group differ in that Tucker et al. (2007) interpreted the timing of deformation as occurring after c. 720 Ma, whereas Collins et al. (2003b) interpreted the nappes as forming before 800–780 Ma, and the upright folding having occurred after the c. 780 Ma intrusive rocks.

The region between the eastern-most part of the transect and the east coast of Madagascar was studied from a structural perspective in Collins et al. (2003a); Nédélec et al. (2000); Raharimahefa and Kusky (2006); Raharimahefa and Kusky (2009); Raharimahefa et al. (2013). Interpretations of this region generally include a D1 event characterised by N-S striking foliations that dip to the west, with a top to the east sense of movement (Collins et al., 2003a; Nédélec et al., 2000). This event is reworked by D2 shear zones such as the Angavo Shear Zone and the Antananarivo virgation zone that underwent low-pressure, granulitic conditions (Nédélec et al., 2000; Paquette and Nédélec, 1998). D3 is characterised by >20 km wide mylonitic high-strain zones and smaller discrete shear zones (Collins et al., 2003a). These dip gently to the west, with a top to the east sense of movement. D4 is characterised by poorly preserved late stage folding (Collins et al., 2003a). Raharimahefa and Kusky (2006); Raharimahefa and Kusky (2009) interpreted three folding events associated with ~N-S striking shear zones along the northeastern and southeastern margins of the Betsimisaraka Suture. A syn-kinematic granite within within the Angavo Shear Zone constrains deformation here to c. 550 Ma (Raharimahefa and Kusky, 2010).

Precise dating of deformation in Madagascar is difficult due to resetting from successive overlapping events. Latest metamorphism in the Anosyen and Androyen domains to the southwest of our study area is constrained to c. 580–520 Ma (Collins et al., 2012; de Wit et al., 2001; Martelat et al., 2000; Paquette et al., 1994) and attributed to high-strain shearing along the Ampanihy and Beraketa shear zones (Boger et al., 2015; Boger et al., 2014). U–Pb dating of zircon rims and titanite have been used to constrain metamorphism in the Itremo Group to c. 550–500 Ma (Tucker et al., 2007). Further east between the eastern-most part of the transect and the east coast of Madagascar, metamorphism has been dated to c. 560–520 Ma (BGS-USGS-GLW, 2008; Collins et al., 2003c; Kröner et al., 2000). From this, it is clear that whatever event was taking place at c. 580–520 Ma, its effects were widespread and resulted in metamorphism in both western and eastern Madagascar.

A comprehensive study of the post-Gondwana history of central Madagascar was undertaken by Emmel et al. (2006), using primarily apatite fission track and titanite fission track analysis. These minerals have closure-temperatures of ~110–60^{o}C (Green et al., 1986) and ~310–265^{o} (Coyle and Wagner, 1998), respectively. This analysis produced ages spanning c. 480–77 Ma, which provides good constraints on the post-tectonic history of Madagascar and the breakup of Gondwana.

In this study we attempt to link up previous structural studies and further extend these interpretations to cover the entire central Madagascar region. We have used remotely sensed data such as satellite imagery and Landsat to interpret the structural framework of central Madagascar, and integrated existing geochronological and structural data. We have ground-truthed this interpretation by collecting structural data and key rock samples for U–Pb zircon, U–Pb apatite, Rb–Sr muscovite and Rb–Sr biotite analysis. This provides a wide range of temperatures from which we can reconstruct the temporal and thermal evolution of this region.

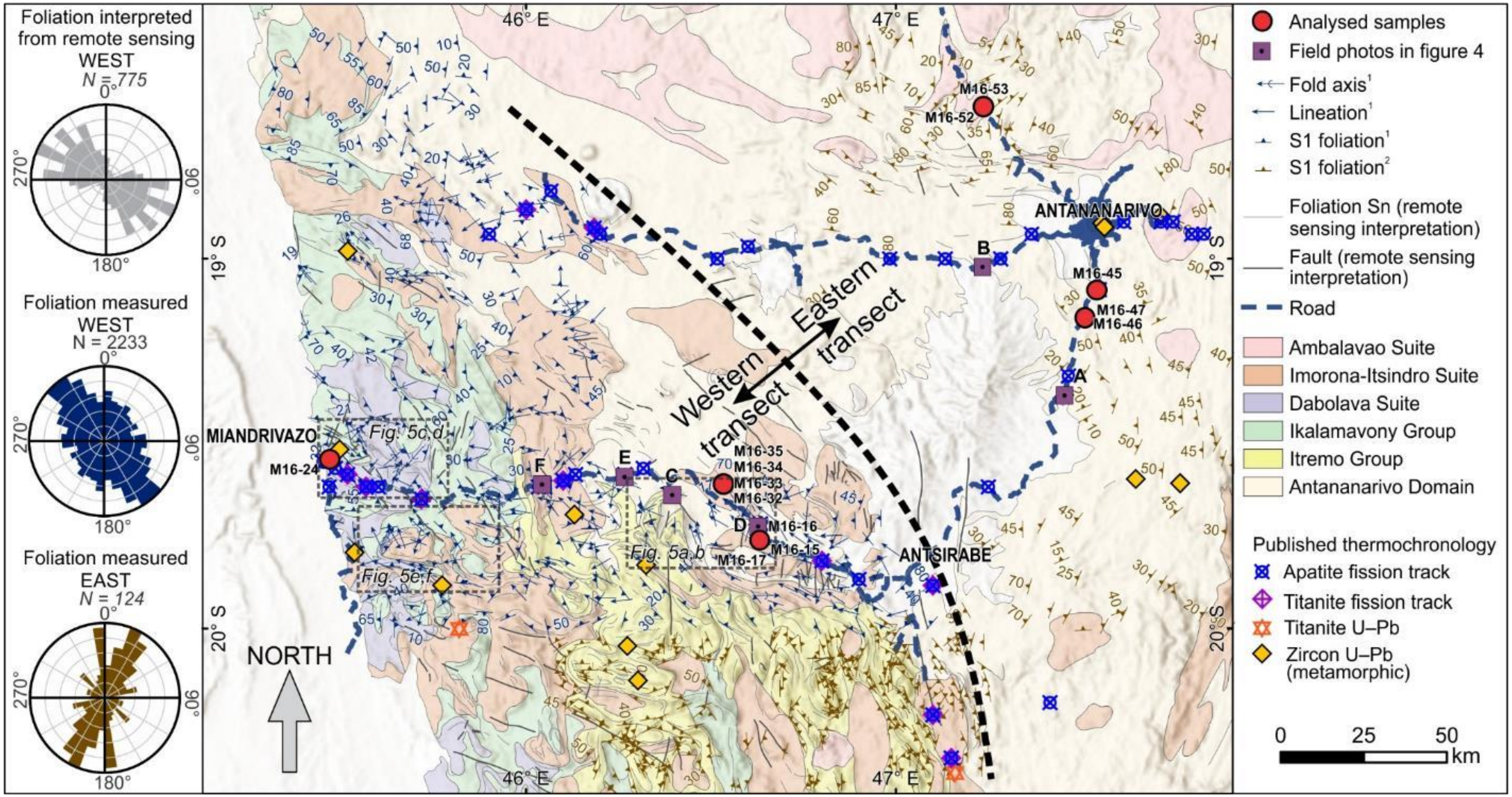

Figure 2 Structural map of central Madagascar with sample locations, photo locations from Figure 4, remote sensing interpretation, structural data from CGS project and 1960's maps (Service Géologique de Madagascar, 1962; Service Géologique de Madagascar, 1963a; Service Géologique de Madagascar, 1963b). Thermochronology data from Emmel et al. (2006); Tucker et al. (2014). Insets for polydeformed folds in Figure 5 also shown. Rose plot calculated from interpretation of foliation (Sn), weighted by polyline length, and rose plots for measured foliations using PolarPlots addin in ArcGIS.

2. Thermochronology

A range of magmatic and orthogneiss samples were collected with the aim of having a representative sample set of the major magmatic suites of central Madagascar. This is important for determining overprinting relationships of key structural events, and determining relative and absolute timing constraints on these events. We used four geochronology/thermochronology techniques: zircon U–Pb (~900–1000°C), apatite U–Pb (~350–550°C), muscovite Rb–Sr (~500–600°C) and biotite Rb–Sr (~300–400°C). Detailed methodology for these techniques is provided in Supplementary file A. Due to the abundance of samples (41 in total), detailed results for each sample and outcrop are also provided in Supplementary file A. Sample descriptions, location and age data are summarised in Table 1 and Figure 3. Isotopic data is given in Supplementary file B.

Table 1 Summary of sample descriptions, outcrop and cross-cutting relationships, and age data. Letters given for each outcrop are the interpreted order of formation/intrusion, based on cross-cutting relationships. All zircon ages are interpreted as magmatic crystallisation ages except for metamorphic ages indicated by (*) and lower intercept ages indicated by (#).

Sample ID	Transect	Outcrop	Sample description	Magmatic Suite	Latitude	Longitude	Elevation (m)	Zircon U–Pb age (Ma)	Apatite U–Pb age (Ma)	Muscovite Rb–Sr age (Ma)	Biotite Rb–Sr age (Ma)
M16-15	West	1/A	Orthogneiss	Betsiboka	-19.7239	46.62736	1067	2456 ± 17	492 ± 5	624 ± 152	528 ± 18
M16-16	West	1/B	Granite	Imorona-Itsindro	-19.7239	46.62736	1067	795 ± 24	498 ± 7	506 ± 82	499 ± 68
M16-17	West	1/C	Pegmatite veins, k-spar rich	Imorona-Itsindro	-19.7239	46.62736	1067	–	494 ± 7	526 ± 39	492 ± 51
M16-24	West	2	k-spar granite	Ambalavao	-19.5443	45.47028	182	576 ± 24	–	519 ± 69	505 ± 59
M16-32	West	3/A	Coarse-grained gneiss	Betsiboka	-19.6107	46.53399	989	2553 ± 24	519 ± 11	446 ± 161	502 ± 20
M16-33	West	3/D	Microgranodioritic dyke-undeformed	Imorona-Itsindro	-19.6107	46.53399	989	798 ± 24	–	–	–
M16-34	West	3/C	Thin dyke intruding M16-32	Betsiboka	-19.6107	46.53399	989	2511 ± 14	515 ± 7	–	–
M16-35	West	3/B	k-spar rich deformed dyke	Betsiboka	-19.6107	46.53399	989	2583 ± 26 2494 ± 14 (*)	502 ± 6	–	513 ± 18
M16-45	East	4	Fine-grained granite	Ambalavao	-19.0869	47.54429	1312	543 ± 18	507 ± 35	–	512 ± 16
M16-46	East	5/A	Orthogneiss	Betsiboka	-19.1599	47.51211	1351	2522 ± 8 543 ± 27 (#)	497 ± 15	604 ± 211	512 ± 24
M16-47	East	5/B	Undeformed cross-cutting granite	Imorona-Itsindro	-19.1599	47.51211	1351	798 ± 48 532 ± 44 (#)	–	657 ± 98	–
M16-52	East	6/A	Grey granite, very weakly foliated	Ambalavao	-18.589	47.23721	1359	568 ± 16	484 ± 14	527 ± 51	511 ± 16
M16-53	East	6/B	Cross-cutting pink granite	Ambalavao	-18.589	47.23721	1359	c. 568	500 ± 10	537 ± 35	521 ± 18

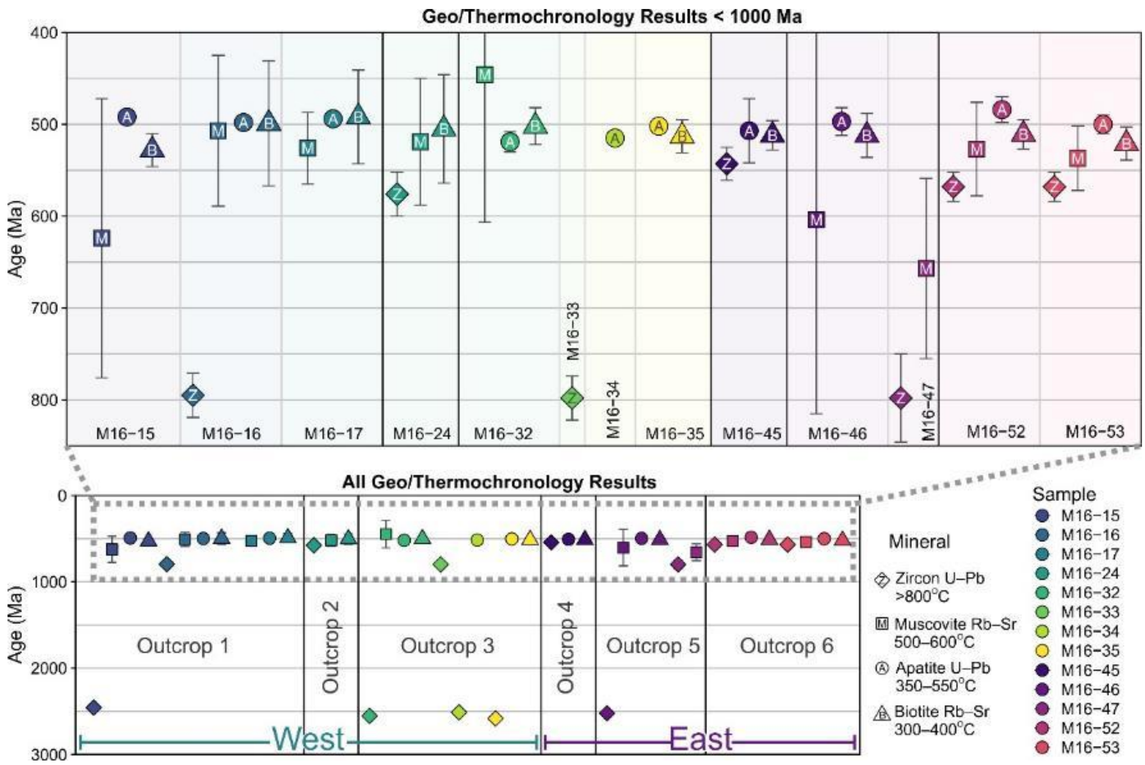

Figure 3 Summary of geo/thermochronology data for each sample and outcrop collected in this study. Error bars are 2σ. Sample locations shown in Figure 2. The bottom figure shows all of the sample data collected, and the top image zooms in on all data that's less than 1000 Ma.

3. Structure of central Madagascar

3.1 Remote sensing methods

We used high resolution aerial imagery and Landsat 8 data to define the structural framework for the study area (Figure 2). Structural trends and lithological boundaries were delineated from the ESRI world imagery basemap and Landsat 8 data in ArcGIS. Structures in the Itremo group are easily identifiable due to relatively low vegetation cover and a strong contrast between quartzites and other rock types. Faults were defined by small offsets in lithologies or as large linear features. Lithologies were identified by similar signals in Landsat data and aerial imagery and boundaries were determined accordingly. Following the identification of major rock packages, lithological trends (S1, S2 etc.) and faults, we were able to identify fold interference patterns and interpret the major deformation events responsible for producing these poly-deformed folds (Figure 5).

3.2 Field methods

Several hundred structural measurements were taken from over 70 localities. Data collected by the Council for Geoscience during the World Bank project in Madagascar was also used, which contains measurements for bedding and foliation. We additionally georeferenced geological maps (Moine, 1968; Service Géologique de Madagascar, 1962; Service Géologique de Madagascar, 1963a; Service Géologique de Madagascar, 1963b) and extracted structural readings. Based on broad lithological and structural styles across the region, we have divided the transect into a western and eastern component. The western transect was conducted along the ~east–west road between Miandrivazo and Antsirabe (west of the dashed line in Figure 2), and the eastern section was conducted along the main road between Antsirabe and ~50 km northwest of Antananarivo (east of the dashed line in Figure 2).

Figure 4 Examples of field outcrops; a) S1 foliation in augen gneiss of the Betsiboka Suite in the Antananarivo Domain, b) S1 foliation in orthogneiss from the Antananarivo Domain, west of Antananarivo, c) flattened conglomerate where S1 is parallel to S0 in the Itremo Group of the Itremo Domain, d) outcrop of foliated gneiss (left) intruded by undeformed granite (right), e) S1 foliation folded around an F2 fold in the Itremo Domain, and f) S1 foliation folding around F2 folds in the Itremo Domain. Locations of field photos shown in Figure 2.

3.3 Western transect

Large-scale structures, fold interference patterns, faults and shear zones are recognisable in remotely sensed data in the western transect region (Figure 5). The Itremo Nappes in the Itremo Domain have been investigated extensively due to their prominence in remotely sensed data and availability of outcrops (Tucker et al., 2007). Here we further extend these interpretations to the Ikalamavony Domain, where identification of lithostratigraphy from remotely sensed data is more difficult, and interpretation is less straightforward. We have integrated our new interpretation from remotely sensed data with new 1:100000 mapping and available structural data (Council for Geosciences, 1:100000 map sheets for Madagascar), to interpret the deformation history of the Ikalamavony and Itremo domains. The strike of S1 fabrics interpreted from remotely sensed data very closely match those measured at outcrops (rose diagrams in Figure 2), we can therefore be confident that our interpretation of S1 structures from remotely sensed data is reliable. The folding of these S1 structures has allowed us to interpret additional deformation events and fold interference patterns. The surface expression of these fold interference patterns has allowed us to interpret the deformation sequence that produced these poly-deformed folds.

3.3.1 D1 Deformation

In remotely sensed data, D1 structures are interpreted by linear or curvilinear trends such as ridges, which we interpret as being representative of the S1 foliation. Quartzite units in particular are easy to recognise in remotely sensed data due to the large contrast in different Landsat bands (e.g. Figure 5). The measured strike of S1 foliations from outcrops closely matches the strikes interpreted from remotely sensed data. The orientation of S1 is dominantly northwest trending in the western transect (see Rose Diagrams in Figure 2).

The first recognisable deformation event at the outcrop scale is defined by a pervasive foliation observed in orthogneisses, paragneisses and metasedimentary rocks (Figure 4a,b,e). In orthogneisses and paragneisses, the foliation is typically defined by the elongation and alignment of biotite, feldspar and quartz. In metasedimentary rocks such as quartzites and marbles, the foliation is sometimes defined by biotite but is often difficult to recognise due to significant recrystallisation of quartz and a lack of other minerals. Primary sedimentary features such as bedding were difficult to recognise in quartzites due to significant recrystallisation. Within the quartzite packages, there are several conglomerate units with large (up to ~5 cm) pebbles (Figure 4c). Here we observe S0 as the interbedded pebble layers, and S1 as the flattening of pebbles.

3.3.2 D2 Deformation

D2 is defined by tight to isoclinal folds with axial traces approximately parallel to S1 in fold limbs. At the outcrop scale we observe these as decimetre- to metre-scale asymmetric, tight to isoclinal folds (Figure 4e,f). F2 folds are similar-type folds, with thickened hinge zones and thinned limbs. An axial planar foliation is difficult to recognise in outcrops, but sometimes occurs as the alignment of biotite in hinge zones. Due to the isoclinal nature of folding, F2 axial traces are approximately parallel to S1 at the regional scale.

F2 folds are recognisable in remotely sensed data as ~500–1000 m wavelength, tight to isoclinal folds. F2 antiforms and synforms are identifiable by the repetition of mapped geological units and constrained by structural measurements. Commonly, F2 folds are refolded during D3 to produce complex fold interference patterns (Figure 5).

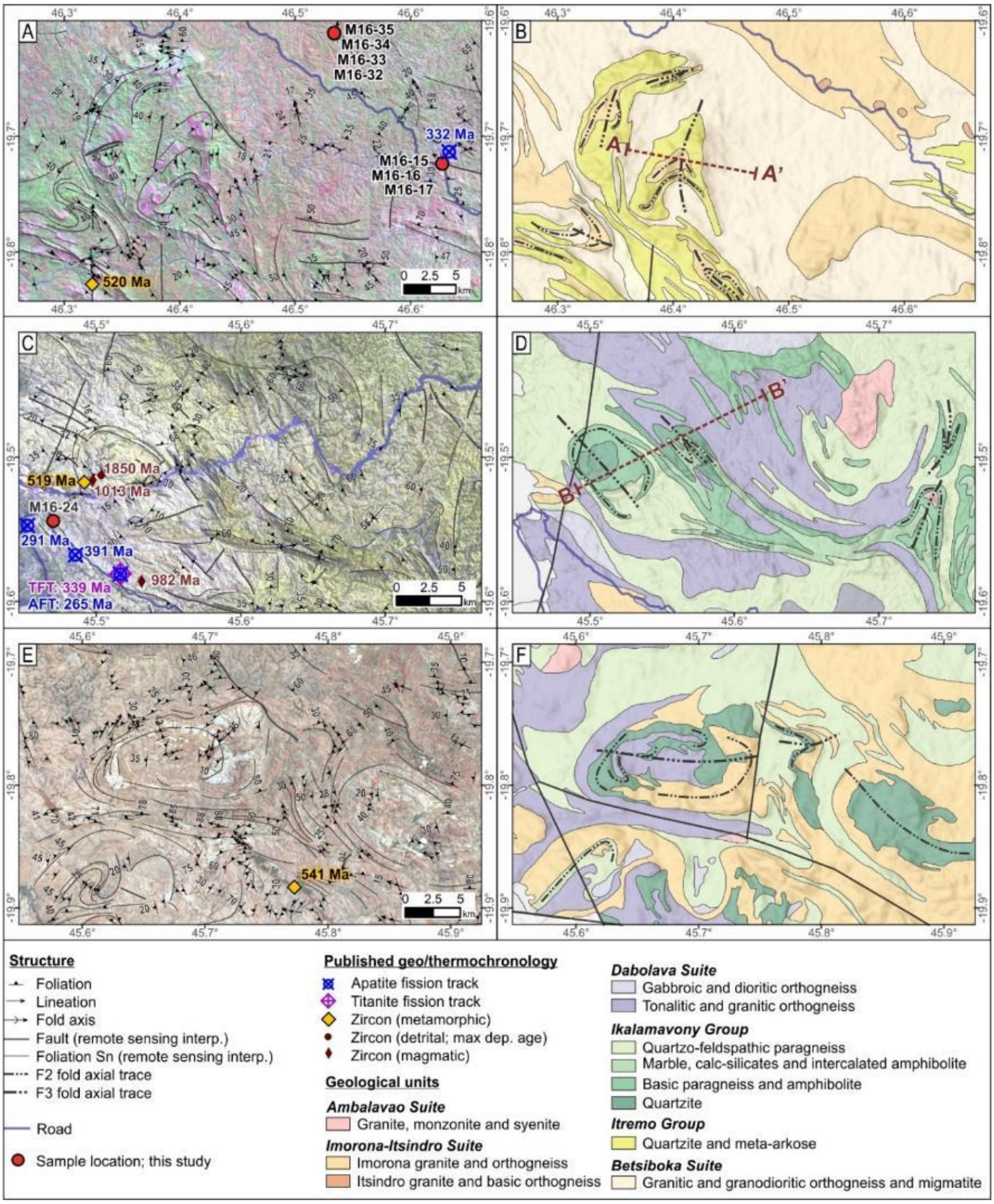

Figure 5 Examples of poly-deformed folds in the Ikalamavony and Itremo domains. A–B: an example of a type 2 fold interference pattern with D2 south-directed recumbent folding overprinted by a F3 north to north-east trending upright fold. C–D: an example of type 2 fold interference patterns with north-west trending third generation upright folds. E–F: an example of a type 1 dome and basin style fold interference pattern. Geological polygons from Council for Geosciences 1:100000 mapsheets.

3.3.3 D3 Deformation and associated fold interference patterns

We do not observe evidence for a third generation deformation event at the outcrop scale, however D3 folds are recognisable in remotely sensed data. The folding of F2 folds during D3 has produced a series of fold interference patterns. Type 1 and type 2 fold interference patterns are observed in remotely sensed data (Figure 5). Type 1 folds occur when an upright folding event is overprinted by an orthogonal upright folding event (Grasemann et al., 2004) and is expressed in Figure 5e,f as the oval structure. Type 2 fold interference patterns occur when a recumbent folding event is orthogonally overprinted by an upright folding event (Grasemann et al., 2004) and is expressed in the first and second locality of Figure 5.

We have constructed two cross-sections of key type 2 fold interference patterns; one from the Itremo Domain and one from the Ikalamavony Domain (Figure 6). We used the QGIS qProf plugin to construct cross-sections. Structural data within ~2 km north or south of the section were included and projected onto the profile. The Africa Digital Elevation Model (30 m resolution) was used to construct the topographic profile.

Cross-section A–A' in Figure 6 represents a type 2 fold interference pattern. Armistead et al. (2018) modelled a structure of very similar geometry and orientation, and showed that this type of feature formed from south-directed, tight, recumbent folding that was orthogonally overprinted by third generation upright folding. In our example from the Itremo Group, the F2 recumbent folding formed during south to slightly south-west directed folding that locally formed by ~north-south shortening. The overprinting F3 upright fold formed during ~east-west shortening that resulted in a north to north-east trending axial trace. These interpreted kinematics are consistent with previous interpretations for deformation in the Itremo Group (Collins et al., 2003b; Tucker et al., 2007).

Adding to the complexity of the structure in A–A' is the juxtaposition of older units (the Archaean Betsiboka Suite) structurally above younger units (Paleoproterozoic Itremo Group). Tucker et al. (2007) observed that the km-scale fold and thrust nappes (our interpreted D2), resulted in the inversion and repetition of Archaean and Proterozoic rocks. This interpretation accounts for why the A–A' section contains older units that appear structurally above younger units.

Cross-section B–B' has F2 folds that are very tight to isoclinal, with axial traces approximately parallel to F3 in F3 fold limbs. In a similar structural regime to A–A', the structures in B–B' formed by ~southeast-directed recumbent folding that was overprinted by a north to northwest trending F3 fold. Given the similarities in structural style between the Itremo and Ikalamavony domains, we suggest that these terranes were juxtaposed prior to deformation and underwent deformation within the same orogenic event.

3.3.4 D4 Deformation

The axial traces of F3 folds vary across the western transect region, as we have shown in the examples of A–A' and B–B' above. Figure 5A–B contains an F3 fold that trends north to northeast, while Figure 5C–D contains several F3 folds that trend more toward the northwest. This is in part due to large wavelength (~30–50 km), open folding post-D3. This event may have occurred in the late stages of folding and thrusting of the Itremo and Ikalamavony domains, or may be related to far-field deformation associated with orogenesis in eastern Madagascar (Collins et al., 2003a).

The general trend of structures varies from the northwest of central Madagascar near Miandrivazo, to the southeast of the study area along the eastern margin of the Itremo Group (Figure 2). Near Miandrivazo (e.g. Figure 5c), D3 axial traces generally trend northwest-southeast. In the Itremo Group and further to the south, these structures are generally north-south trending. This trend broadly follows the curve of our transect boundary line between the western and eastern transects delineated in Figure 2. This regional variation may relate to D4 deformation or may relate to orogenic bending as orogenesis progressed.

3.3.5 Regional variation in deformation

Complex fold interference patterns are more easily identifiable in the westernmost region of the western transect and in the Itremo Group. Deformation intensity appears to weaken toward the east, with an absence of complex fold interference patterns between Antsirabe and Antananarivo. The Imorona-Itsindro Suite in particular becomes progressively less deformed to the east. In the west, the Imorona-Itsindro Suite is folded into fold interference patterns, whereas in the east it only appears to be folded into weakly-defined F3 folds. This is consistent with our sampling of c. 850–750 Ma rocks along this weakly deformed margin, where rock samples appear undeformed or very weakly deformed.

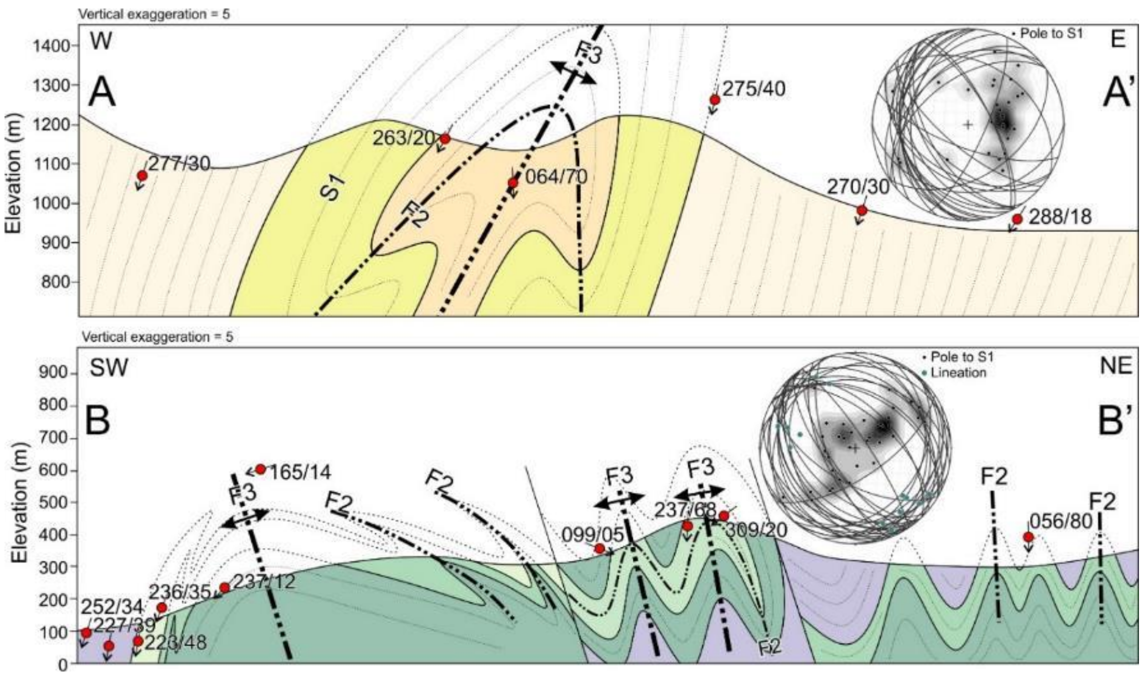

Figure 6 Geological cross-sections of transects labelled in Figure 5. Sections generated using QProf plugin in QGIS. Structural measurements (dip direction/dip) within ~2km of the section are projected along the profile. Topographic profile derived from 30 arc-second DEM of Africa (USGS).

3.4 Eastern transect

The eastern transect was conducted along the ~north-south road between Antsirabe and Antananarivo, and further to the north of Antananarivo (Figure 2). This transect largely intersects Cenozoic extrusive volcanics and the Archaean Betsiboka Suite. Generally, deformation in the eastern transect is much less intense compared to the western transect, and we observe fewer deformation events (Figure 2). Here we only identify a primary foliation (S1), with no later deformation events recognised.

3.4.1 D1 Deformation

Much like the western transect, at the outcrop scale we observe a pervasive foliation within the Antananarivo orthogneisses, which we interpret as an S1 foliation. The foliation is commonly preserved by the alignment of biotite, feldspar and quartz in orthogneisses. Structural measurements from Service Géologique de Madagascar (1963a) and Service Géologique de Madagascar (1963b) indicate that S1 foliations between Antsirabe and Antananarivo dominantly strike ~north-northeast, with dips moderately to the west (see Rose Diagram in Figure 2). North of Antananarivo, S1 is more variable, following the Antananarivo virgation zone (e.g. Nédélec et al., 2000).

4. Discussion

4.1 Deformation sequence

The earliest phase of deformation that we observe is a pervasive foliation in magmatic rocks, orthogneisses and metasedimentary rocks. In the western transect, this S1 foliation is then folded into F2 folds that are tight to isoclinal, asymmetric, similar-type folds. These folds range in scale from decimetre- to kilometre-scale and are observable at the outcrop scale and from remotely sensed data. F2 folds have been subsequently deformed during D3 and D4, however their original orientation would have been preserved with ~east-west striking axial traces. Further south where structures are more north-south trending, Tucker et al. (2007) interpreted east or south-east directed vergence from these fold trends. We suggest these folding events developed as the result of ~northeast-southwest shortening (present day orientation), with ~south to southwest-directed vergence.

F2 folds are folded during D3 to produce Type 1 and Type 2 fold interference patterns (Figure 5, Figure 6). The axial traces of F3 folds vary across the region, indicating a subsequent D4 event that gently folded existing folds. The majority of F3 fold axial traces are ~north-south striking, and orthogonally overprint F2 folds. We therefore interpret D3 as a ~east-west shortening event. Together, D2 and D3 have produced the fold interference patterns observable in remotely sensed data.

Type 1 and Type 2 fold interference patterns are common in fold and thrust belts, and more commonly form during progressive deformation rather than discrete deformation events. We therefore suggest that D2 and D3 in the western transect most likely formed during the same orogenic event, through progressive deformation. As pointed out in Tucker et al. (2007), these folds are east-verging and were likely produced within a zone of west-dipping convergence (present day direction).

4.2 Spatial variation of deformation

In order to attribute deformation events to orogenesis, we need to understand the spatial variation of deformation. The fold interference patterns we have described above are not present everywhere in the map extent. These strongly deformed sequences are only present in the southwest of the study area in the western transect, in the Ikalamavony Domain and Itremo Domain. The road between Antsirabe and point 'E' in Figure 2 approximately marks the boundary between high intensity deformation to the southwest and relatively undeformed, or weakly deformed terranes to the northeast of this boundary. This is consistent with our observations from outcropping c. 850–750 Ma rocks where we observe them as undeformed along the main road in this zone of low intensity deformation. Other authors have interpreted these rocks as strongly deformed further to the south (e.g. Archibald et al., 2016), where we interpret poly-deformed folds from remotely sensed data.

To the east of Antsirabe, there is a distinct change in structural trend. In the 'western transect' region, there is an overall northwest strike trend to structures. In the 'eastern transect', the structural trends vary from the northern part of the transect to the southern part of the transect, with structures trending ~west, north of Antananarivo (near samples M16-52 and M16-53), and north or north-east trending between Antananarivo and Antsirabe. These structures were studied in detail in Collins et al. (2003a); Nédélec et al. (2000); Raharimahefa and Kusky (2006); Raharimahefa and Kusky (2009); Raharimahefa et al. (2013).

4.3 Temporal constraints on deformation

4.3.1 Relative timing of deformation

Understanding the ages of geological units that are deformed and undeformed can help constrain the timing of deformation. At the regional scale in the western transect, the c. 850–750 Ma Imorona-Itsindro Suite is poly-deformed, and therefore was intruded prior to the onset of at least D2 and D3. In the eastern transect and in the region studied by Collins et al. (2003a); Nédélec et al. (2000); Raharimahefa and Kusky (2006); Raharimahefa and Kusky (2009), the Imorona-Itsindro Suite is not poly-deformed into complex fold interference patterns but instead is elongated along the length of the c. 550 Ma Angavo shear zone. This suggests that different structural regimes are responsible for deformation in the west and east.

In the western transect, the c. 550 Ma Ambalavao Suite is undeformed and therefore provides a minimum age constraint on deformation here. In the east, the Ambalavao Suite is represented by both deformed and undeformed rocks. We therefore suggest that deformation in the west occurred between c. 750 and c. 550 Ma, which is consistent with interpretations by Tucker et al. (2007). Deformation in eastern Madagascar likely occurred later at c. 550 Ma, which is consistent with age determinations for the Angavo Shear Zone and Antananarivo virgation zone (Meert et al., 2003; Nédélec et al., 2000; Paquette and Nédélec, 1998; Raharimahefa and Kusky, 2010).

4.3.2 Thermochronology

We have used minerals with a range of closure temperatures in an attempt to capture different stages of the tectonic evolution of Madagascar. Our sampling included the major magmatic suites of Madagascar, including the c. 2500 Ma Antananarivo Domain orthogneisses, the c. 850–750 Ma Imorona-Itsindro Suite, and the c. 550 Ma Ambalavao Suite (Table 1). Interestingly, apatite U–Pb ages—which record the age the minerals were cooled through ~350–550°C (Chamberlain and Bowring, 2001; Schoene and Bowring, 2007)—are all c. 500 Ma regardless of their magmatic crystallisation age. Muscovite and biotite, which have Rb–Sr closure temperatures of ~500–600°C (Armstrong et al., 1966) and ~300–400°C (Del Moro et al., 1982; Jenkin et al., 2001; Verschure et al., 1980) respectively, also record ages of c. 500 Ma. This implies that the final stages of orogenesis in Madagascar, regardless of whether this was in the west or east, affected the entire central region of the island, where rocks were heated to at least ~500°C.

Multiple thermochronometers have provided insights into the medium-temperature thermo-tectonic evolution across the western and eastern part of Madagascar. As we have shown here, the more recent c. 550 Ma event affected the entire island such that it cooled synchronously through ~500–300°C at c. 500 Ma. The c. 550–500 Ma regional thermal perturbation would have overprinted prior events, obscuring any evidence of a pre-existing thermo-tectonic evolution. Using thermochronometers that record temperatures higher than ~600°C (e.g. allanite U–Pb or monazite U–Pb) in future research may be able to provide further constraints on the timing of orogenesis, particularly in the distal regions, where temperatures during the c. 550 Ma event may not have been hot enough to cause complete reset. Without direct dating of the structures observed, we need to look further afield for evidence of subduction and collision that resulted in deformation of central Madagascar.

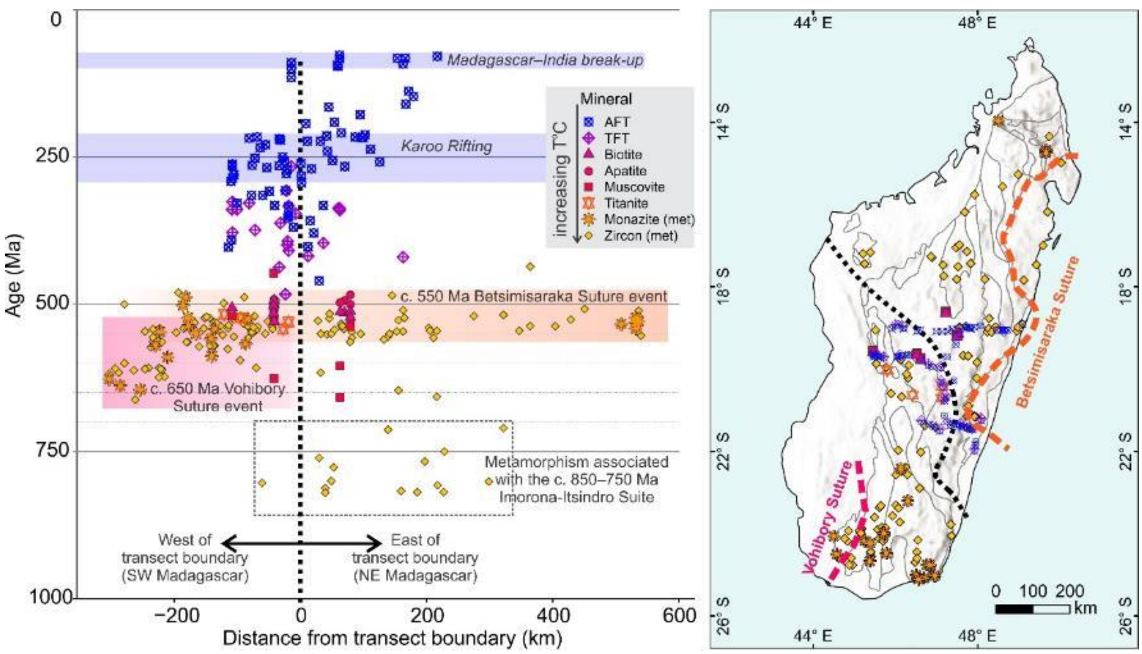

Figure 7 Summary of new thermochronology data and published metamorphic data. Biotite, apatite and muscovite are from this study. Metamorphic minerals zircon, monazite and titanite are from the compilation of Tucker et al. (2014). Apatite fission track (AFT), titanite fission track (TFT) and associated interpretations of Phanerozoic rifting are from Emmel et al. (2006). Locations of data points shown in the map to the right, terranes are the same as those from Figure 1b.

4.4 Gondwana collision in Madagascar

Due to a widespread event that reset medium-temperature thermochronometers like apatite, muscovite and biotite at c. 500 Ma—recording the timing of older active subduction in western Madagascar is difficult to reconcile. Since structural data suggest a west over east sense of thrusting and folding, we suggest that the subduction zone would have been west-dipping, consistent with the interpretation of Tucker et al. (2007). This also suggests that a >550 Ma suture zone must be to the west of our study area. Looking westward from the Ikalamavony Domain, the boundaries between the Anosyen, Androyen and Vohibory terranes (Figure 1b) present possible suture zones that resulted in complex folding in the Ikalamavony and Itremo domains.

The Anosyen Domain contains siliciclastic sedimentary rocks with predominantly c. 2400–1600 Ma detrital zircons, with a dominant age peak at c. 1850 Ma (Boger et al., 2014). This detrital zircon signature is indistinguishable from the Itremo Domain (Costa et al., Submitted; Cox et al., 1998). This suggests a stratigraphic continuum between the Anosyen and Itremo domains. The Anosyen and Itremo domains were interpreted as the same passive margin sequence to the Antananarivo Craton by Boger et al. (2014), and therefore, we do not consider the Itremo-Anosyen boundary as a tectonic boundary.

The Beraketa high-strain zone between the Anosyen and Androyen domains was interpreted as a suture zone by Boger et al. (2015) that closed at c. 580–520 Ma. This interpretation was based on c. 630–600 Ma metamorphism restricted to the west of this high-strain zone, and widespread c. 580–520 Ma magmatism and metamorphism on both sides of the high-strain zone. In this model, the subduction zone was east-dipping (present day direction), and resulted in the syn- to post-tectonic Ambalavao granites throughout Madagascar. However, the structures we have described and those described by Tucker et al. (2007) require a ~west-dipping (top to the east; present day direction) sense of movement, making an east-dipping subduction zone beneath the Antananarivo Craton at this time unlikely.

These authors interpreted that another west-dipping subduction zone was active beneath the Vohibory Domain until c. 650 Ma, and that collision between the Vohibory Domain and Androyen Domain occurred at c. 630–610 Ma, outboard from the Antananarivo Craton. In this model, subduction was west-dipping.

Much like the Itremo Group and metasedimentary groups within the Anosyen Domain, the Androyen Domain also hosts several groups of Paleoproterozoic metasedimentary rocks, as well as intrusive rocks dated to c. 2090–2020 Ma, c. 1790 Ma and c. 920 Ma (Boger et al., 2015). In our view, the difference between the Androyen and Anosyen domains is not as distinct as Boger et al. (2015) suggest, and instead we propose that the Androyen Domain is more closely correlated with the Anosyen and Itremo domains. While the Androyen-Anosyen boundary may indeed be a suture zone, we suggest that the Androyen-Vohibory boundary separates terranes of very distinct origin, and is therefore more likely to be the major Gondwana suture zone in western Madagascar. Metamorphism is also widespread either side of this boundary at c. 650–600 Ma, which likely constrains the age of collision (Figure 7, Figure 8b).

We therefore propose that the Androyen-Vohibory suture marked by the Ampanihy high-strain zone was responsible for high intensity deformation and polydeformed folds in the Ikalamavony and Itremo domains. This would have been a west-dipping suture (present day direction), resulting in the emplacement of the c. 630 Ma Marosavoa Suite in the Vohibory Domain. Metamorphism of this age is also recorded in the Androyen Domain (Figure 7, Figure 8b).

Magmatism and metamorphism at c. 550 Ma is widespread throughout Madagascar and marks the final assembly of Gondwana in Madagascar (Figure 7; Figure 8). In the eastern part of the transect, c. 550 Ma Ambalavao granites are deformed and sheared along a north-south trending Angavo shear zone (Nédélec et al., 2000; Raharimahefa and Kusky, 2010). Due to their deformed nature in the east and undeformed nature in the west, we suggest the c. 550 Ma event more closely aligns with the proposed Betsimisaraka Suture in eastern Madagascar, which amalgamated Madagascar with the Dharwar Craton of India (Armistead et al., 2017; Collins, 2006; Collins and Windley, 2002). Furthermore, geochronological and metamorphic evidence from the Angavo Shear Zone and Antananarivo virgation zone in eastern Madagascar, imply low-pressure granulitic conditions (Nédélec et al., 2000) at c. 550 Ma (Raharimahefa and Kusky, 2010)—consistent with the timing of the Betsimisaraka Suture.

Medium-temperature thermochronometers analysed in this study reveal ages of c. 500 Ma. We interpret these to represent the waning stages of the Betsimisaraka Suture and East African Orogen, and mark the termination of orogenesis in Madagascar and subsequent cooling. The Phanerozoic post-tectonic history of Madagascar is recorded by apatite and titanite fission track ages (Emmel et al., 2006). These show a cooling trend from c. 500 Ma, with a peak in apatite fission track at c. 250 Ma marking Karoo rifting, and another apatite fission track peak at c. 100 Ma, which marks the breakup of Madagascar and India (Emmel et al., 2006)(Figure 7).

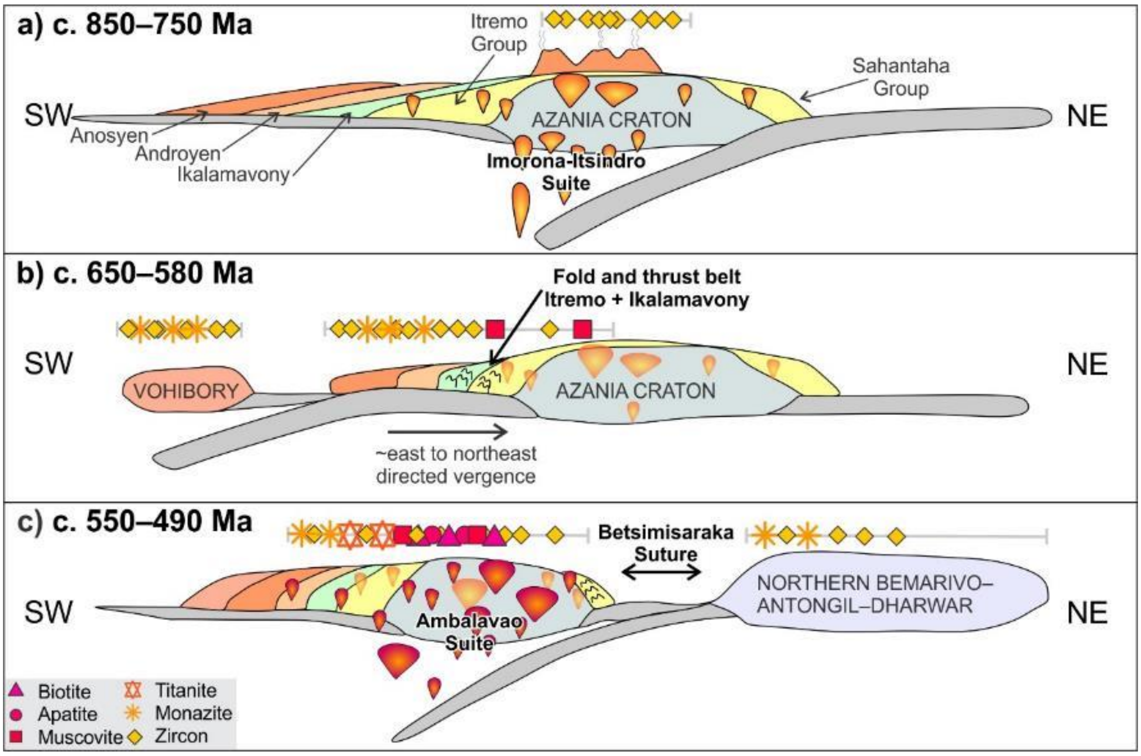

Figure 8 Schematic diagram of the Neoproterozoic evolution of Madagascar, showing approximate locations of analysed and compiled thermochronology/metamorphic data from Figure 7. Modified after Armistead et al. (In Review).

4.5 Conclusions

We have integrated structural analysis with medium-temperature thermochronology to constrain the timing of orogenic events in Madagascar. We observe complex fold interference patterns in both the Ikalamavony and Itremo domains. We suggest these formed in response to ~southwest-dipping subduction beneath the Vohibory Domain at c. 650 Ma. North-south trending structures in eastern Madagascar formed in response to the ~west-dipping c. 550 Ma Betsimisaraka Suture, which resulted in the emplacement of widespread granitic rocks and the resetting of medium-temperature minerals throughout much of central Madagascar. We have shown the power of using U–Pb apatite to date the cooling stages of orogenesis, as well as the potential for Rb–Sr mica dating to provide useful thermochronological constraints.

Acknowledgments

- Paul Macey, CGS structural data
- Renée Tamblyn is thanked for helpful discussion about the Rb–Sr data
- SA is funded by an Australian government PhD Scholarship and AC is funded by an Australian Research Council Future Fellowship FT120100340. This forms TRaX Record ### and is a contribution to IGCP projects 628 (Gondwana Map) and 648 (Supercontinent Cycles and Global Geodynamics).

References

Archibald, D.B., Collins, A.S., Foden, J.D., Payne, J.L., Holden, P., Razakamanana, T., De Waele, B., Thomas, R.J. and Pitfield, P.E.J., 2016. Genesis of the Tonian Imorona–Itsindro magmatic Suite in central Madagascar: Insights from U–Pb, oxygen and hafnium isotopes in zircon. Precambrian Research, 281: 312-337.

Armistead, S.E., Betts, P.G., Ailleres, L., Armit, R.J. and Williams, H.A., 2018. Cu-Au mineralisation in the Curnamona Province, South Australia: A hybrid stratiform genetic model for Mesoproterozoic IOCG systems in Australia. Ore Geology Reviews, 94: 104-117.

Armistead, S.E., Collins, A., Payne, J.L., Cox, G.M., Merdith, A.S., Foden, J.D., Razakamanana, T. and De Waele, B., In Review. Evolving marginal terranes during Neoproterozoic supercontinent reorganisation: constraints from the Bemarivo Belt in northern Madagascar. Tectonics.

Armistead, S.E., Collins, A.S., Payne, J.L., Foden, J.D., De Waele, B., Shaji, E. and Santosh, M., 2017. A re-evaluation of the Kumta Suture in western peninsular India and its extension into Madagascar. Journal of Asian Earth Sciences.

Armstrong, R.L., Jäger, E. and Eberhardt, P., 1966. A comparison of K-Ar and Rb-Sr ages on Alpine biotites. Earth and Planetary Science Letters, 1(1): 13-19.

BGS-USGS-GLW, 2008. Republique de Madagascar Ministère de L'engergie et des Mines (MEM/SG/DG/UCP/PGRM). British Geological Survey Research Report.

Boger, S.D., Hirdes, W., Ferreira, C.A.M., Jenett, T., Dallwig, R. and Fanning, C.M., 2015. The 580–520Ma Gondwana suture of Madagascar and its continuation into Antarctica and Africa. Gondwana Research, 28(3): 1048-1060.

Boger, S.D., Hirdes, W., Ferreira, C.A.M., Schulte, B., Jenett, T. and Fanning, C.M., 2014. From passive margin to volcano–sedimentary forearc: The Tonian to Cryogenian evolution of the Anosyen Domain of southeastern Madagascar. Precambrian Research, 247: 159-186.

Chamberlain, K.R. and Bowring, S.A., 2001. Apatite–feldspar U–Pb thermochronometer: a reliable, mid-range (~450°C), diffusion-controlled system. Chemical Geology, 172(1): 173-200.

Collins, A.S., 2006. Madagascar and the amalgamation of Central Gondwana. Gondwana Research, 9(1-2): 3-16.

Collins, A.S., Fitzsimons, I.C.W., Hulscher, B. and Razakamanana, T., 2003a. Structure of the eastern margin of the East African Orogen in central Madagascar. Precambrian Research, 123(2–4): 111-133.

Collins, A.S., Johnson, S., Fitzsimons, I.C., Powell, C.M., Hulscher, B., Abello, J. and Razakamanana, T., 2003b. Neoproterozoic deformation in central Madagascar: a structural section through part of the East African Orogen. Geological Society, London, Special Publications, 206(1): 363-379.

Collins, A.S., Kinny, P.D. and Razakamanana, T., 2012. Depositional age, provenance and metamorphic age of metasedimentary rocks from southern Madagascar. Gondwana Research, 21(2-3): 353-361.

Collins, A.S., Kröner, A., Fitzsimons, I.C.W. and Razakamanana, T., 2003c. Detrital footprint of the Mozambique ocean: U–Pb SHRIMP and Pb evaporation zircon geochronology of metasedimentary gneisses in eastern Madagascar. Tectonophysics, 375(1-4): 77-99.

Collins, A.S. and Pisarevsky, S.A., 2005. Amalgamating eastern Gondwana: The evolution of the Circum-Indian Orogens. Earth-Science Reviews, 71(3-4): 229-270.

Collins, A.S., Razakamanana, T. and Windley, B.F., 2000. Neoproterozoic extensional detachment in central Madagascar: implications for the collapse of the East African Orogen. Geological Magazine, 137(1): 39-51.

Collins, A.S. and Windley, B.F., 2002. The tectonic evolution of central and northern Madagascar and its place in the final assembly of Gondwana. The Journal of geology, 110(3): 325-339.

Costa, R.L., Schmitt, R.S., Collins, A., Armistead, S.E., Razakamanana, T. and Archibald, D., Submitted. Tectonic evolution of an Early Cryogenian synmagmatic basin in central Madagascar. Precambrian Research.

Cox, R., Armstrong, R.A. and Ashwal, L.D., 1998. Sedimentology, geochronology and provenance of the Proterozoic Itremo Group, central Madagascar, and implications for pre-Gondwana palaeogeography. Journal of the Geological Society, 155(6): 1009-1024.

Coyle, D. and Wagner, G., 1998. Positioning the titanite fission-track partial annealing zone. Chemical Geology, 149(1-2): 117-125.

De Waele, B., Thomas, R.J., Macey, P.H., Horstwood, M.S.A., Tucker, R.D., Pitfield, P.E.J., Schofield, D.I., Goodenough, K.M., Bauer, W., Key, R.M., Potter, C.J., Armstrong, R.A., Miller, J.A., Randriamananjara, T., Ralison, V., Rafahatelo, J.M., Rabarimanana, M. and Bejoma, M., 2011. Provenance and tectonic significance of the Palaeoproterozoic metasedimentary successions of central and northern Madagascar. Precambrian Research, 189(1-2): 18-42.

de Wit, M.J., Bowring, S.A., Ashwal, L.D., Randrianasolo, L.G., Morel, V.P.I. and Rambeloson, R.A., 2001. Age and tectonic evolution of Neoproterozoic ductile shear zones in southwestern Madagascar, with implications for Gondwana studies. Tectonics, 20(1): 1-45.

Del Moro, A., Puxeddu, M., di Brozolo, F.R. and Villa, I.M., 1982. Rb-Sr and K-Ar ages on minerals at temperatures of 300°–400° C from deep wells in the Larderello geothermal field (Italy). Contributions to Mineralogy and Petrology, 81(4): 340-349.

Emmel, B., Jacobs, J., Kastowski, M. and Graser, G., 2006. Phanerozoic upper crustal tectono-thermal development of basement rocks from central Madagascar: An integrated fission-track and structural study. Tectonophysics, 412(1-2): 61-86.

Emmel, B., Jons, N., Kroner, A., Jacobs, J., Wartho, J.A., Schenk, V., Razakamanana, T. and Austegard, A., 2008. From Closure of the Mozambique Ocean to Gondwana Breakup: New Evidence from Geochronological Data of the Vohibory Terrane, Southwest Madagascar. The Journal of Geology, 116(1): 21-38.

Fernandez, A., Schreurs, G., Villa, I.M., Huber, S. and Rakotondrazafy, M., 2003. Age constraints on the tectonic evolution of the Itremo region in Central Madagascar. Precambrian Research, 123(2-4): 87-110.

Fitzsimons, I.C.W. and Hulscher, B., 2005. Out of Africa: detrital zircon provenance of central Madagascar and Neoproterozoic terrane transfer across the Mozambique Ocean. Terra Nova, 17(3): 224-235.

Grasemann, B., Wiesmayr, G., Draganits, E. and Fusseis, F., 2004. Classification of refold structures. The Journal of geology, 112(1): 119–125.

Green, P., Duddy, I., Gleadow, A., Tingate, P. and Laslett, G., 1986. Thermal annealing of fission tracks in apatite: 1. A qualitative description. Chemical Geology: Isotope Geoscience section, 59: 237-253.

Jenkin, G.R.T., Ellam, R.M., Rogers, G. and Stuart, F.M., 2001. An investigation of closure temperature of the biotite Rb-Sr system: The importance of cation exchange. Geochimica et Cosmochimica Acta, 65(7): 1141-1160.

Jöns, N. and Schenk, V., 2007. Relics of the Mozambique Ocean in the central East African Orogen: evidence from the Vohibory Block of southern Madagascar. Journal of Metamorphic Geology, 0(0): 071115150845002-???

Jöns, N. and Schenk, V., 2011. The ultrahigh temperature granulites of southern Madagascar in a polymetamorphic context: implications for the amalgamation of the Gondwana supercontinent. European Journal of Mineralogy, 23(2): 127-156.

Kröner, A., Hegner, E., Collins, A.S., Windley, B.F., Brewer, T.S., Razakamanana, T. and Pidgeon, R.T., 2000. Age and magmatic history of the Antananarivo Block, central Madagascar, as derived from zircon geochronology and Nd isotopic systematics. American Journal of Science, 300(4): 251-288.

Martelat, J.-E., Lardeaux, J.-M., Nicollet, C. and Rakotondrazafy, R., 2000. Strain pattern and late Precambrian deformation history in southern Madagascar. Precambrian research, 102(1-2): 1-20.

Meert, J.G., Nédélec, A. and Hall, C., 2003. The stratoid granites of central Madagascar: paleomagnetism and further age constraints on neoproterozoic deformation. Precambrian Research, 120(1-2): 101-129.

Merdith, A.S., Collins, A.S., Williams, S.E., Pisarevsky, S., Foden, J.D., Archibald, D.B., Blades, M.L., Alessio, B.L., Armistead, S. and Plavsa, D., 2017. A full-plate global reconstruction of the Neoproterozoic. Gondwana Research, 50: 84-134.

Moine, B., 1968. Massif Schisto-Quartzo-Dolomitique: Reion d'Ambatofinandrahana centre-ouest du socle cristallin precambrien de Madagascar In: N. Sciences de la terre (Editor). Centre de l'Institut Géographique National à Tananarive.

Moine, B., Bosse, V., Paquette, J.-L. and Ortega, E., 2014. The occurrence of a Tonian–Cryogenian (~850Ma) regional metamorphic event in Central Madagascar and the geodynamic setting of the Imorona–Itsindro (~800Ma) magmatic suite. Journal of African Earth Sciences, 94: 58-73.

Nédélec, A., Ralison, B., Bouchez, J.L. and Grégoire, V., 2000. Structure and metamorphism of the granitic basement around Antananarivo: A key to the Pan-African history of central Madagascar and its Gondwana connections. Tectonics, 19(5): 997-1020.

Paquette, J.-L. and Nédélec, A., 1998. A new insight into Pan-African tectonics in the East–West Gondwana collision zone by U–Pb zircon dating of granites from central Madagascar. Earth and Planetary Science Letters, 155(1-2): 45-56.

Paquette, J.-L., Nédélec, A., Moine, B. and Rakotondrazafy, M., 1994. U-Pb, single zircon Pb-evaporation, and Sm-Nd isotopic study of a granulite domain in SE Madagascar. The Journal of Geology, 102(5): 523-538.

Raharimahefa, T. and Kusky, T.M., 2006. Structural and remote sensing studies of the southern Betsimisaraka Suture, Madagascar. Gondwana Research, 10(1-2): 186-197.

Raharimahefa, T. and Kusky, T.M., 2009. Structural and remote sensing analysis of the Betsimisaraka Suture in northeastern Madagascar. Gondwana Research, 15(1): 14-27.

Raharimahefa, T. and Kusky, T.M., 2010. Temporal evolution of the Angavo and related shear zones in Gondwana: Constraints from LA-MC-ICP-MS U–Pb zircon ages of granitoids and gneiss from central Madagascar. Precambrian Research, 182(1-2): 30-42.

Raharimahefa, T., Kusky, T.M., Toraman, E., Rasoazanamparany, C. and Rasaonina, I., 2013. Geometry and kinematics of the late Proterozoic Angavo Shear Zone, Central Madagascar: Implications for Gondwana Assembly. Tectonophysics, 592: 113-129.

Schoene, B. and Bowring, S.A., 2007. Determining accurate temperature–time paths from U–Pb thermochronology: An example from the Kaapvaal craton, southern Africa. Geochimica et Cosmochimica Acta, 71(1): 165-185.

Schofield, D.I., Thomas, R.J., Goodenough, K.M., De Waele, B., Pitfield, P.E.J., Key, R.M., Bauer, W., Walsh, G.J., Lidke, D.J. and Ralison, A.V., 2010. Geological evolution of the Antongil Craton, NE Madagascar. Precambrian Research, 182(3): 187-203.

Service Géologique de Madagascar, T., 1962. Moramanga-Brickaville.

Service Géologique de Madagascar, T., 1963a. Antsirabe-Ampatolampy

Service Géologique de Madagascar, T., 1963b. Miarinarivo-Tanarive.

Thomas, R.J., De Waele, B., Schofield, D.I., Goodenough, K.M., Horstwood, M., Tucker, R., Bauer, W., Annells, R., Howard, K., Walsh, G., Rabarimanana, M., Rafahatelo, J.M., Ralison, A.V. and Randriamananjara, T., 2009. Geological evolution of the Neoproterozoic Bemarivo Belt, northern Madagascar. Precambrian Research, 172(3-4): 279-300.

Tucker, R., Ashwal, L., Handke, M., Hamilton, M., Le Grange, M. and Rambeloson, R., 1999. U-Pb geochronology and isotope geochemistry of the Archean and Proterozoic rocks of north-central Madagascar. The Journal of Geology, 107(2): 135-153.

Tucker, R., Roig, J.-Y., Delor, C., Amelin, Y., Goncalves, P., Rabarimanana, M., Ralison, A. and Belcher, R., 2011. Neoproterozoic extension in the Greater Dharwar Craton: a reevaluation of the “Betsimisaraka suture” in Madagascar. Canadian Journal of Earth Sciences, 48(2): 389-417.

Tucker, R.D., Kusky, T.M., Buchwaldt, R. and Handke, M.J., 2007. Neoproterozoic nappes and superposed folding of the Itremo Group, west-central Madagascar. Gondwana Research, 12(4): 356-379.

Tucker, R.D., Roig, J.Y., Moine, B., Delor, C. and Peters, S.G., 2014. A geological synthesis of the Precambrian shield in Madagascar. Journal of African Earth Sciences, 94: 9-30.

Verschure, R.H., Andriessen, P.A.M., Boelrijk, N.A.I.M., Hebeda, E.H., Maijer, C., Priem, H.N.A. and Verdurmen, E.A.T., 1980. On the thermal stability of Rb-Sr and K-Ar biotite systems: Evidence from coexisting Sveconorwegian (ca 870 Ma) and Caledonian (ca 400 Ma) biotites in SW Norway. Contributions to Mineralogy and Petrology, 74(3): 245-252.